Edelweiss Applied Science and Technology
ISSN: 2576-8484
Vol. 9, No. 6, 2244-2260
2025
Publisher: Learning Gate
DOI: 10.55214/25768484.v9i6.8364

Numerical study on the performance of combined Darrirus-Savonius vertical axis wind turbine

Farhan A. Khammas[1*], Rand Nabil[2]
[1]Department of Unmanned Aerial Vehicle (UAV) Engineering. Collage of Engineering, Al-Nahrain University, Jadriya, Baghdad, Iraq; far_1961ah@yahoo.com (F.A.K.).
[2]Department of Mechanical Engineering, Collage of Engineering, Al-Nahrain University, Jadriya, Baghdad, Iraq.

Abstract: CFD simulations were conducted for these types of wind rotors to address the increasing focus of scholars in the renewable energy sector on studying the adoption of sustainable energy sources and reducing fossil fuel consumption. Vertical axis wind turbines (VAWTs) have become increasingly prevalent for wind power generation. This work presents a computational analysis of the performance of a vertical-axis wind turbine for three designs using Fluent 2020 R2 CFD software. The three designs' three-dimensional computational fluid dynamics (CFD) were compared using the k-epsilon augmented wall treatment as a turbulence model at an airflow velocity of 5 m/s. From this study, it can be concluded that it is possible to use this type of hybrid wind turbine in areas with low wind speeds due to their quick response to rotation. For these reasons, this type of hybrid wind turbine can be used in residential areas as a practical application, since these areas are characterized by low wind speeds in most cases.

Keywords: *CFD, K-epsilon, Combined blade, Power generation, Wind Turbine.*

1. Introduction

The continuous development and expansion of wind power is an essential technology that can both meet people's energy needs and stop greenhouse gas emissions from causing significant local weather variations. Because of its superior technology and favorable economics, experts predict that wind energy will make up 5% of the world's power market by 2020 [1]. Over the past ten years, the average cumulative growth rate of wind power capacity worldwide has exceeded 30 percent [2]. The improvement of wind turbine applied sciences allowed wind power to perform a relevant step forward and the local manufacturing of smooth electric power. It renewed the pastime in vertical-axis wind turbines (VAWTs) for small-scale electricity generation [3, 4].

The low power coefficient and a low potential factor of the VAWTs, it has awesome and great advantages, such as low development fee and low renovation fee because of the generator and gearbox on the ground. Also, no need for yaw mechanism, any pressure, or herbal course pointers because they catch the wind in any path and capacity to take blessings of gusty and turbulent winds. Moreover, much less noise and avian issues and of route they can be gathered more intently in wind farms so growing the generated electricity per unit of land vicinity [5]. The VAWTs are considered important types because they represent another good option for generating energy [6]. For this reason, in recent times, a large group of researchers have been conducted on straight-bladed wind turbines (SB-VAWT) due to their special advantages [7, 8] such as ease of manufacture, low cost, ease of maintenance and upkeep [9]. VAWTs are receiving wind from all directions. This leads to their not needing a guidance system during operation. Computational

History: Received: 2 April 2025; Revised: 4 June 2025; Accepted: 9 June 2025; Published: 25 June 2025
* Correspondence: far_1961ah@yahoo.com

fluid dynamics (CFD) modeling in aerodynamics applications is common, the possibility of improving the power of a wind turbine by combining two types of wind turbines to take advantage of the positive aspects of each task and thus leading to a significant increase in the area in contact with the air and thus increasing the torque and thus increasing the power output of the combined wind turbine. The application of computational fluid dynamics (CFD) in many engineering fields, including automotive [10] biomedicine [11] heat transfer [12, 13] wind energy [2, 14] and many others.

The previous experiments conducted on Darius-Savonius integrated wind turbines have shown that their energy coefficient is much higher than the energy coefficient of the Savonius turbine alone, as the aerodynamic performance is closely related to the shape (design) such as the type and number of blades used, the tip speed, etc., and in all that has not been evaluated yet. The research is still on the effect of the type and number of blades on the aerodynamic properties of the integrated wind turbine.

Farhan and Omar [15] conducted a study on the distinctive design shapes of wind turbine blades, including Savonius blades and Darius composite blade, to obtain the leading value of the drag force per blade. Execution Tip Speed Ratio (TSR) accurately predicting effectiveness is the focus of many WT investigations Biadgo, et al. [16]. Farhan [17] Investigate numerically how the combined blade area affects the drag coefficient, initial torque, and power coefficient in order to boost the VAWT's overall power output. In this research paper, the performance of the Darius-Savonius integrated turbine for source [18] was analyzed computationally using CFD program.

2. Physical Model

The combined wind turbine proposed in the present study consist of 3- combined blade Savonius - Darrieus. Three Savonius buckets were placed next to three SB Darrieus (NACA 0012), with a height of 11 cm, Savonius buckets with 5.6 cm in diameter, 0.2 cm in thickness, and 11 cm in height. The distance between the Savonius and the shaft is 2.75 cm. However, the space held between Savonius and Darrieus is 1.54 m, the shaft diameter is 0.5 cm [18] as shown in Figure 1.

Both Savonius and Darrieus were fixed horizontally by using upper and lower board, which is 2mm in thickness and 11 cm in diameter as shown in Figure 2.

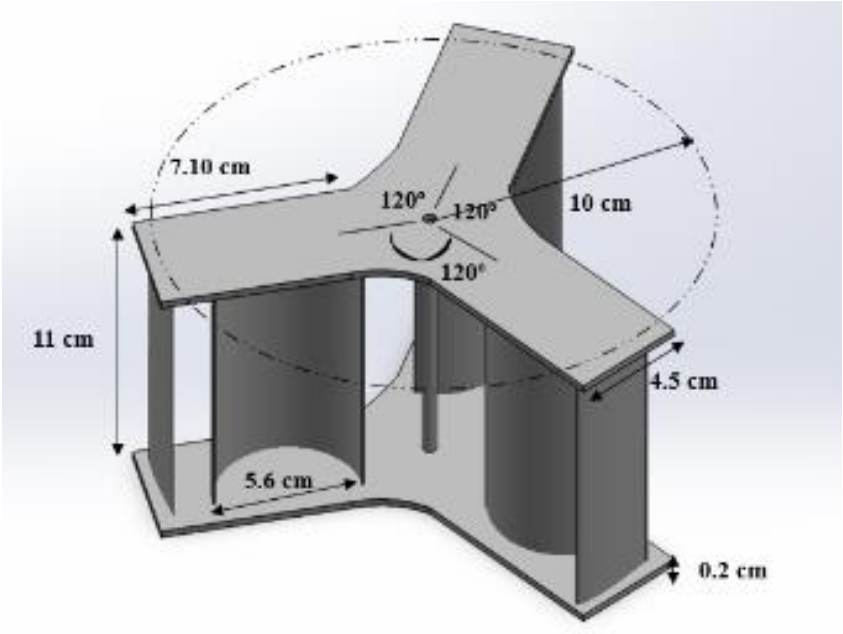

Figure 1.
Combined Darrieus-Savonius turbine.

Edelweiss Applied Science and Technology
ISSN: 2576-8484
Vol. 9, No. 6: 2244-2260, 2025
DOI: 10.55214/25768484.v9i6.8364

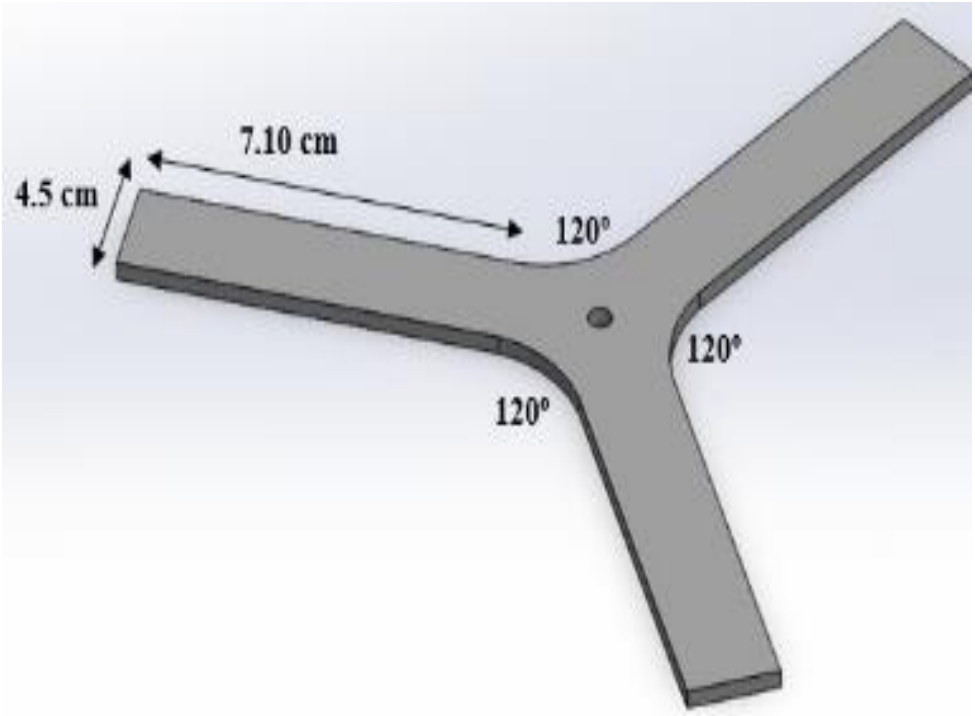

Figure 2.
Upper and lower board.

3. CFD Formulation for the Boundary Condition and Hybrid Savonius-Darrieus Rotor

The turbine geometries have been modeled using SolidWorks 2021, and then imported to ANSYS FLUENT 2020 R2 for simulation purposes. Turbines have been surrounded by a box that represents a wind tunnel with 30×30×40 cm in dimensions.

In order to investigate the complementary impact of both Savonius and Darrieus turbines, each turbine has been individually modeled and simulated using the same predetermined dimensions,

The left side of the box has been set as the "inlet" velocity inlet boundary condition where 5 m/sec has been used as wind speed and the right side "outlet" as pressure outlet condition. However, the walls of the turbines are considered "walls" as illustrated in Figure 3.

Edelweiss Applied Science and Technology
ISSN: 2576-8484
Vol. 9, No. 6: 2244-2260, 2025
DOI: 10.55214/25768484.v9i6.8364

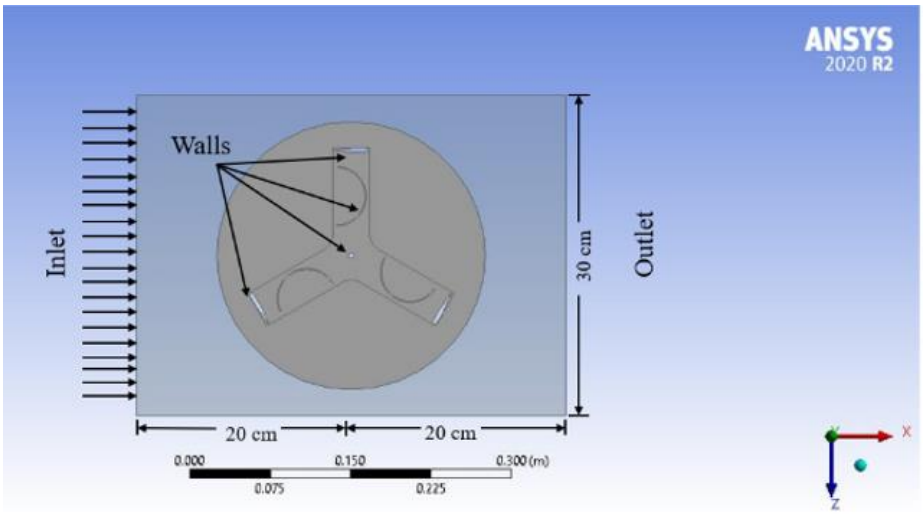

Figure 3.
Boundary conditions for turbines computational domain.

For incompressible flow and constant viscosity governing equations for Navier-Sokes can be given as: The following turbulence kinetic energy equations are the SST k-ω governing equations used to solve this problem.

$$\frac{\partial}{\partial t}(\rho k) + \frac{\partial}{\partial x_i}(\rho k u_i) = \frac{\partial}{\partial x_i}\left[\left(\mu + \frac{\mu_t}{\sigma_k}\right)\frac{\partial k}{\partial x_j}\right] + G_k + G_b - \rho\mathcal{E} - Y_M + S_k \quad (1)$$

$$\frac{\partial}{\partial t}(\rho \mathcal{E}) + \frac{\partial}{\partial x_i}(\rho \mathcal{E} u_i) = \frac{\partial}{\partial x_j}\left[\left(\mu + \frac{\mu_t}{\sigma_\varepsilon}\right)\frac{\partial \mathcal{E}}{\partial x_j}\right] + C_{1\varepsilon}\frac{\mathcal{E}}{k}(G_k + C_{3\varepsilon}G_b) - C_{2\varepsilon}\rho\frac{\mathcal{E}^2}{k} + S_\varepsilon \quad (2)$$

The value of five constants of the standard k- $\mathcal{E}$ turbulence model are taken as:

$$C_\mu = 0.09\,,\quad C_{1\mathcal{E}} = 1.44\,,\quad C_{2\mathcal{E}} = 1.44\,,\quad \sigma_k = 1.0\,,\quad \sigma_\mathcal{E} = 1.3$$

4. Computational Modeling

The geometries have been examined by Fluent 2020 R2 software. As well as, meshing the proposed case. The wind tunnel frame was constructed with structured mesh, while both blades and containers were constructed with unstructured mesh, as shown in figure 4. However, fine mesh has been focused on concave and convex faces. The spinning component was carried out using an unstructured mesh, while the wind fixed part (box) was constructed using a structured mesh.

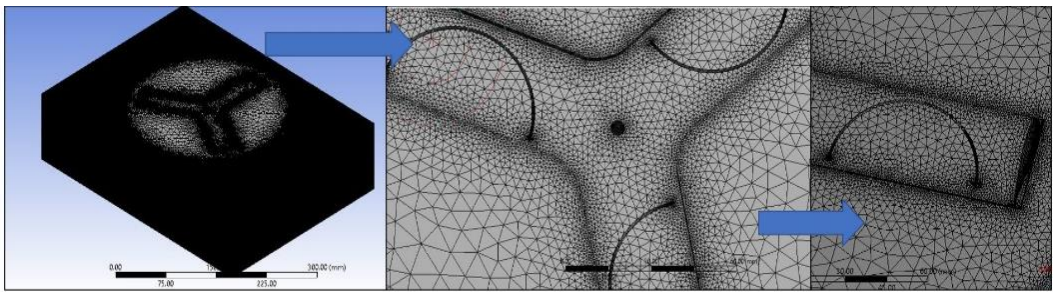

Figure 4.
Generated Mesh for Combined Wind turbine.

The number of cells has been increased by fining the mesh many times and considering an output parameter (Torque T) until the impact of condensing the mesh is negligible, as shown in Table 1.

Condensing mesh level 5 has been set for the last runs as illustrated forwarding the other two levels has a micro difference for the output parameter (T).

Table 1.
Illustration of the Condensing mesh level of the combined wind turbine.

Condensing mesh level	Cells Number	Output parameter (Torque)
1	4602796	0.062111593
2	4129807	0.062045438
3	3920357	0.061985587
4	3802336	0.061920646
5	3750919	0.061889177
6	3713796	0.061844866
7	3688927	0.0618233

The mesh independence for combined wind turbine as shown in Figure 5.

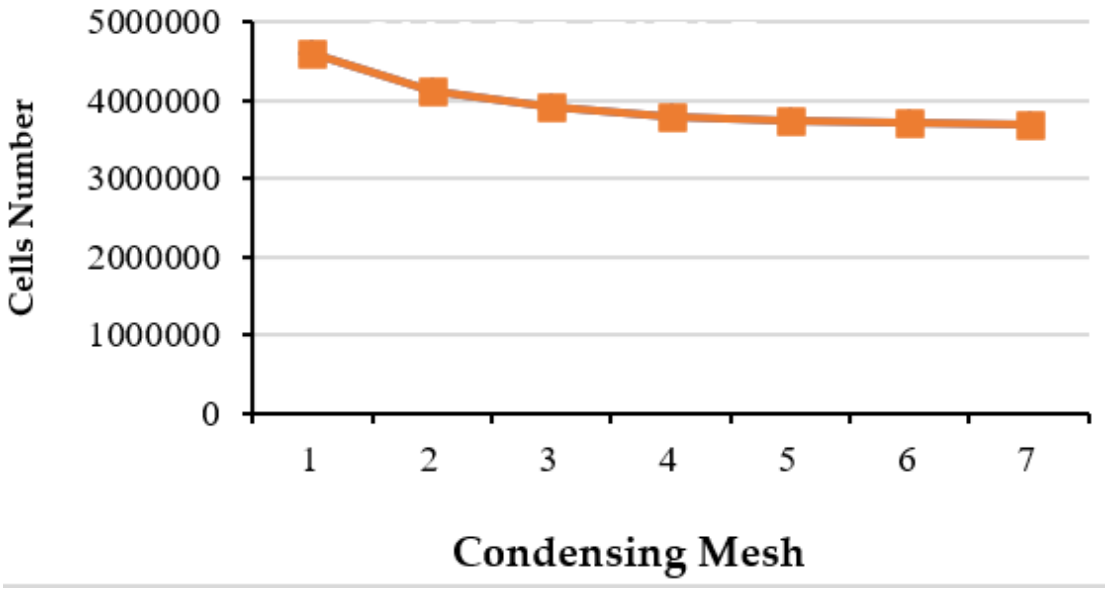

Figure 5.
Mesh Independence.

The continuity and turbulence equations, as well as the finite difference versions of the Navier-Stokes equation, were solved using Fluent 2020 R2 CFD software. The conventional k-ε turbulence model with an enhanced wall function was chosen. In this study, the dynamic grid or rotating reference frame technique is implemented [17]. This study focused on a single rotating reference system that revolves proportionately to the incoming fluid stream, including its buckets, blades, and central axis. The SIMPLE algorithm was a sequential procedure used to control all of the numerical parameters. A second order upwind interpolating technique was used to obtain accurate solutions for the convective components of the momentum equations and the turbulence equations.

5. Assessment of the Hybrid Savonius-Darrieus Wind Turbine Contour

Pressure and velocity contour graphs were produced by the CFD simulations for the Darrieus wind turbine and jointed 3- bladed Savonius with 3-bladed Darrieus wind turbine. The simulations were conducted with a wind speed of 5m/sec. Figures (6, 7, 8, and 9) illustrates pressure contour, velocity contour, dynamic pressure and total pressure respectively for cases without and with the combination.

Edelweiss Applied Science and Technology
ISSN: 2576-8484
Vol. 9, No. 6: 2244-2260, 2025
DOI: 10.55214/25768484.v9i6.8364

Figure 6 presents an investigation of the static pressure distribution inside the contour structure of both a single blade rotor and a coupled blade rotor. Investigation of this distribution indicates that the static pressure attains its maximum magnitude at the forefront of each blade. The static pressure is reduced to its lowest level at the same location on the blade's reverse side. Although the minimal difference is shown for Darrieus, the combined rotor exhibits a much high value. Therefore, the lift generation increases.Thus, reducing the reverse torque increases the overall positive torque of the wind turbine. The production of electricity rises as a result. This clarifies how the integrated blade area affects a (VAWT) initial torque, power factor, and total power production when the integrated blade technology is used.

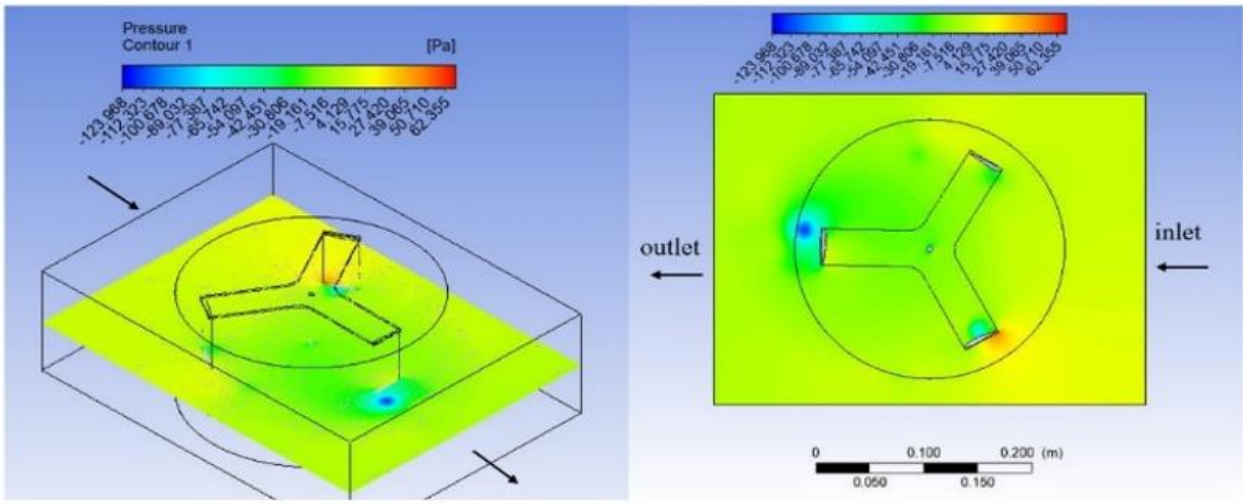

(a)

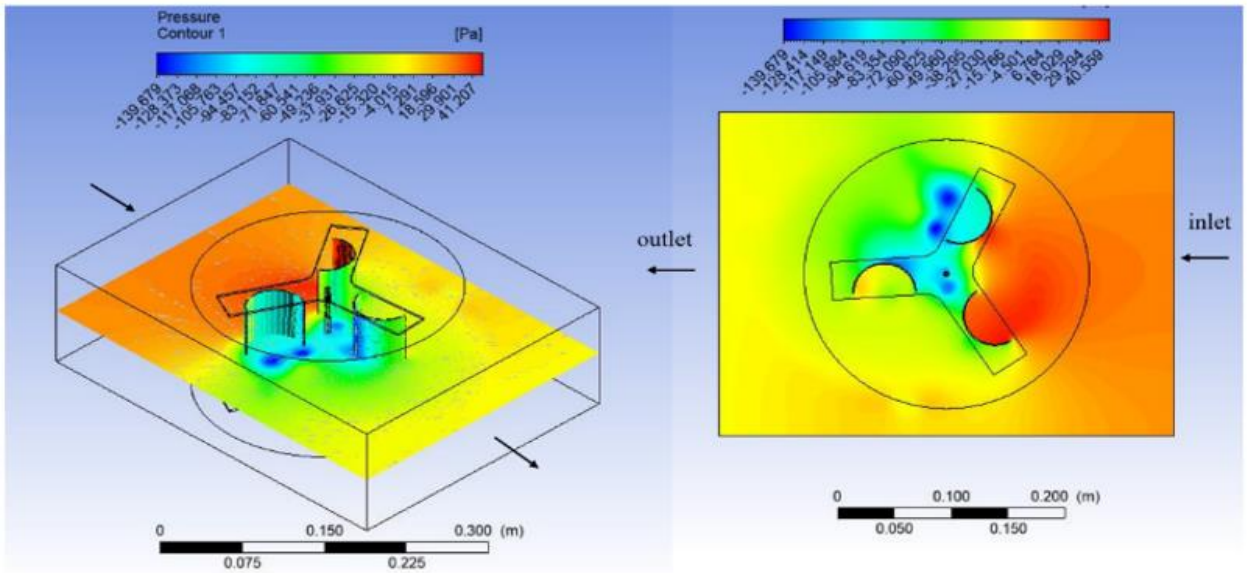

(b)

Edelweiss Applied Science and Technology
ISSN: 2576-8484
Vol. 9, No. 6: 2244-2260, 2025
DOI: 10.55214/25768484.v9i6.8364

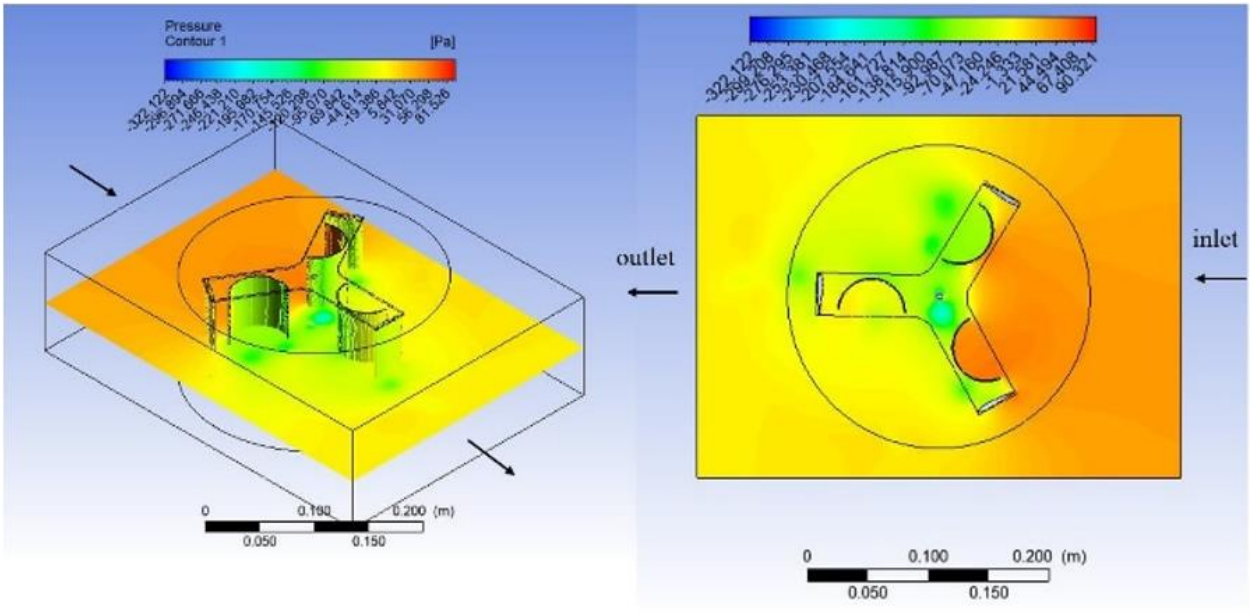

Figure 6.
Pressure contour for wind turbine type (a) Darruis 3S-blades (b) Savonius (c) combined (Darrieus - Savonius).

Upon passing over the downstream blades, it was observed that the flow increased, reaching a maximum value almost double the velocity of the flow upstream due to the position of blades in 90º facing the stream as illustrated in Figure 7.

A rise in the velocity differential between the bucket's two sides in a Darrieus-bladed turbine results in a higher generation of power in the direction of the wind speed, as shown in figure7 (a). However, it has been observed that the velocity range of the combined turbine reduced as a result of the inclusion of Savonius blades, as shown in figure7 (c). There exists a significant barrier to the flow of air in this region, apart from the blades. As a result, there is a rise in both the drag force and the rotational speed of the main shaft of the turbine. The wind turbine can generate more power as a result of producing more energy overall.

Edelweiss Applied Science and Technology
ISSN: 2576-8484
Vol. 9, No. 6: 2244-2260, 2025
DOI: 10.55214/25768484.v9i6.8364

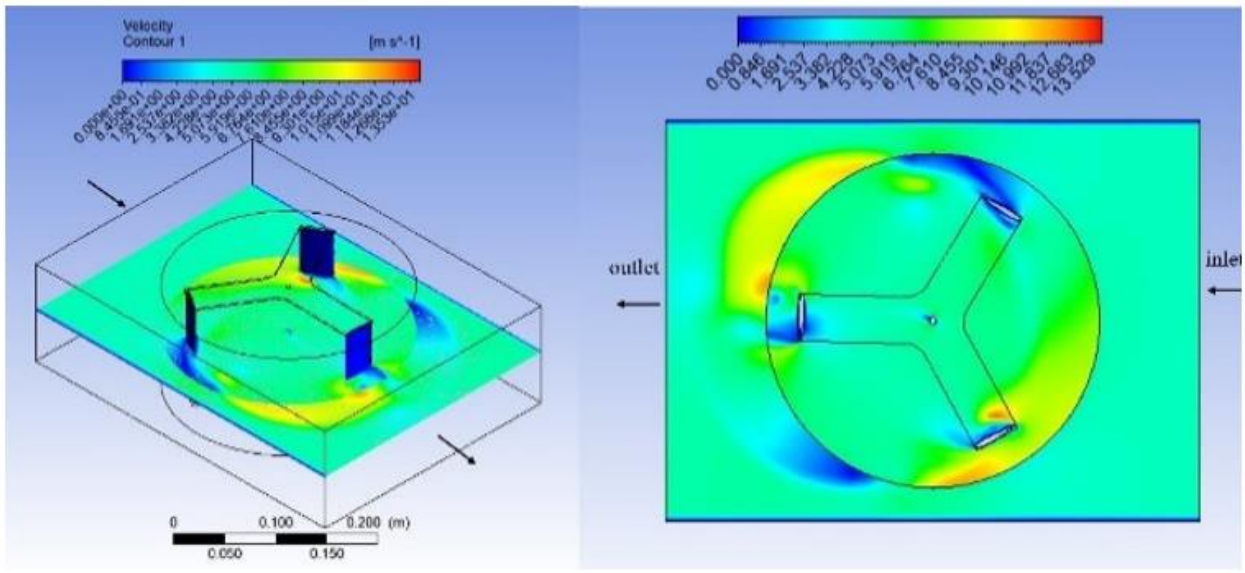

(a)

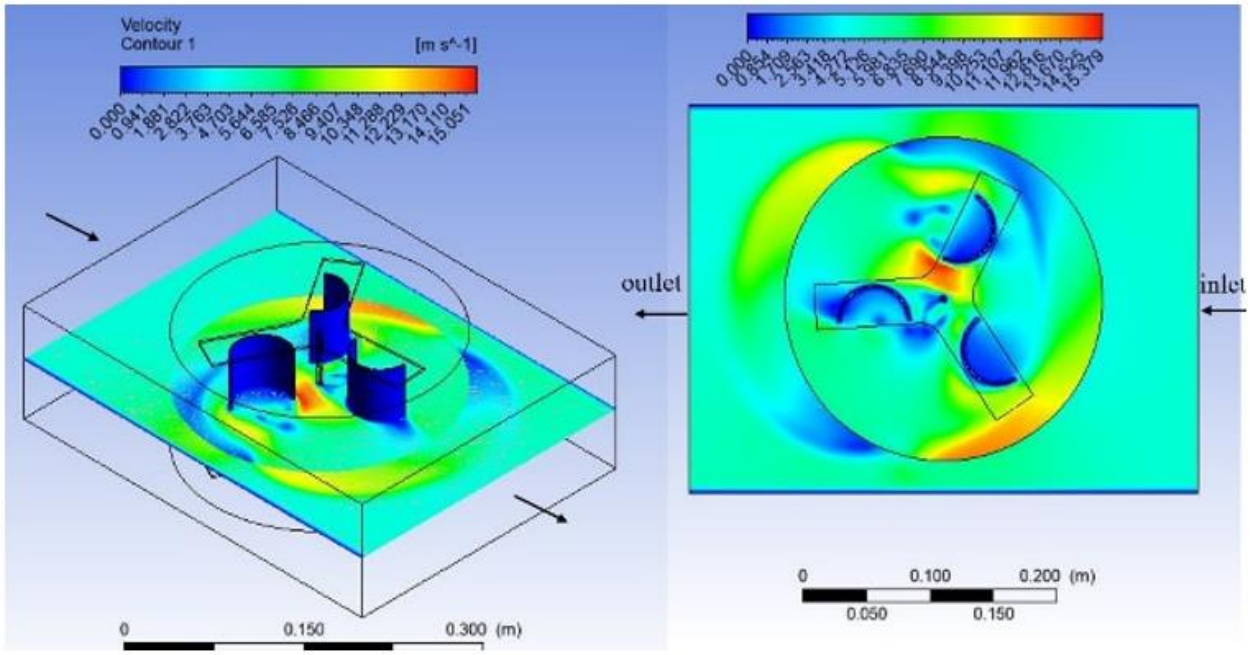

(b)

Edelweiss Applied Science and Technology
ISSN: 2576-8484
Vol. 9, No. 6: 2244-2260, 2025
DOI: 10.55214/25768484.v9i6.8364

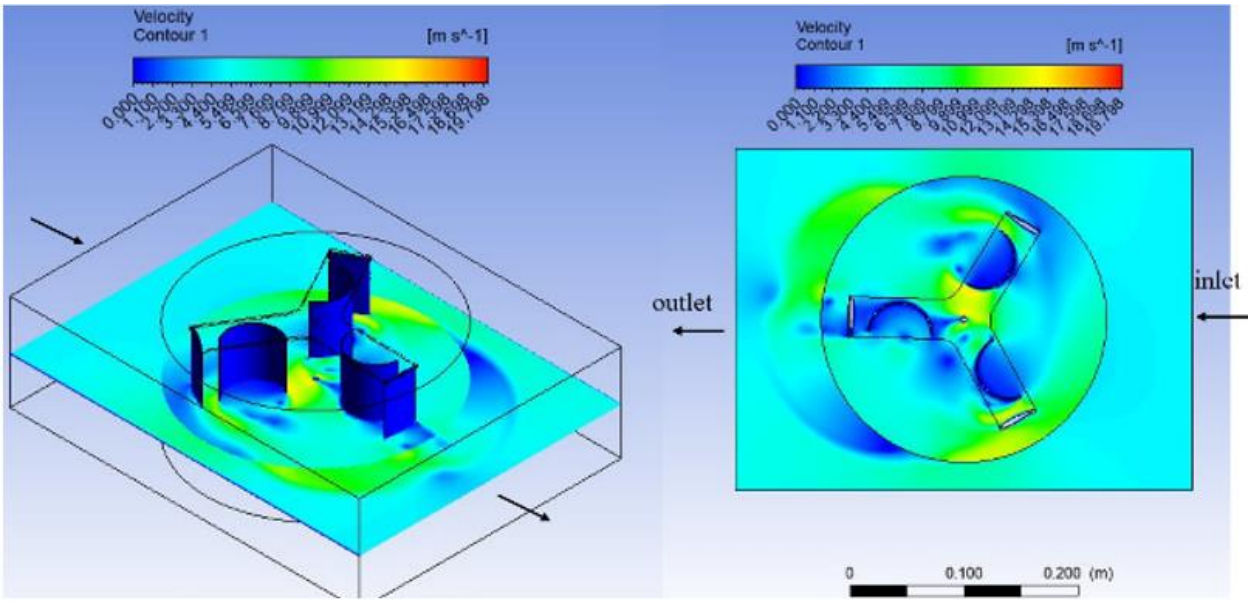

Figure 7.
Velocity contour for wind turbine type (a) Darruis 3S-blades (b) Savonius (c) combined (Darrieus - Savonius).

In dynamic pressure plots, the upper part has the maximum value that responsible for increasing the aerodynamics characteristics. However, the area around Savoinus bucket was observed to have its highest value. The collision of separate vortices from the bucket's convex surface with the Darrieus blade may be the cause of the dynamic pressure increase that was seen on the convex side of the bucket. Figure 8 illustrated the dynamic pressure contour

Edelweiss Applied Science and Technology
ISSN: 2576-8484
Vol. 9, No. 6: 2244-2260, 2025
DOI: 10.55214/25768484.v9i6.8364

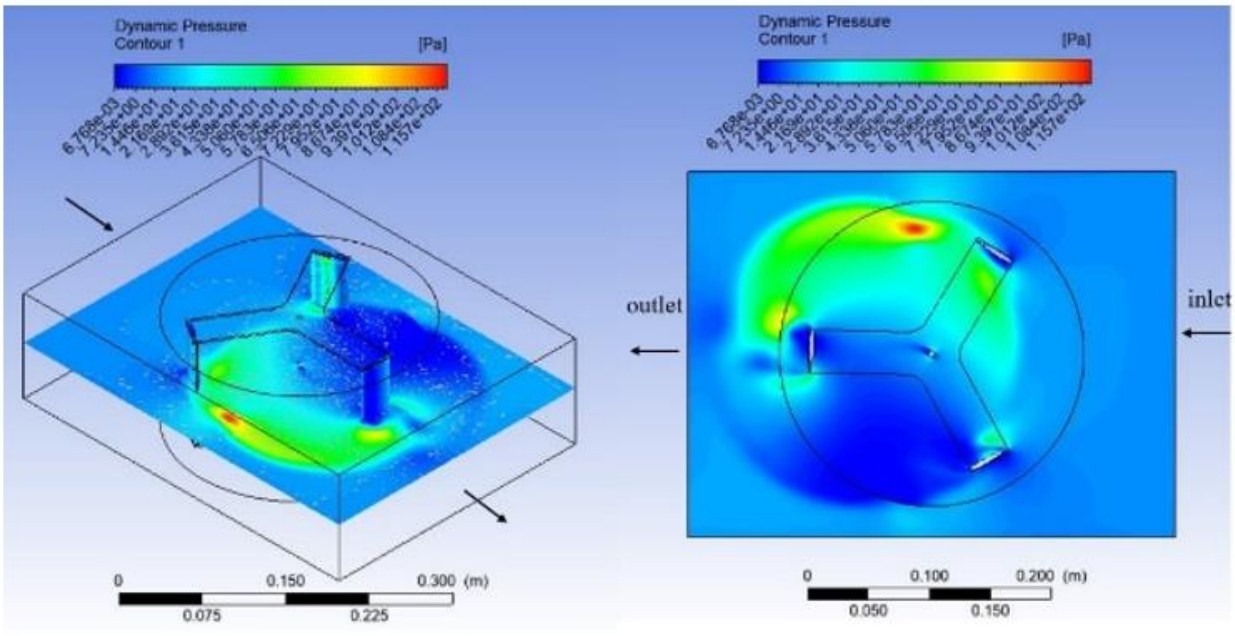

(a)

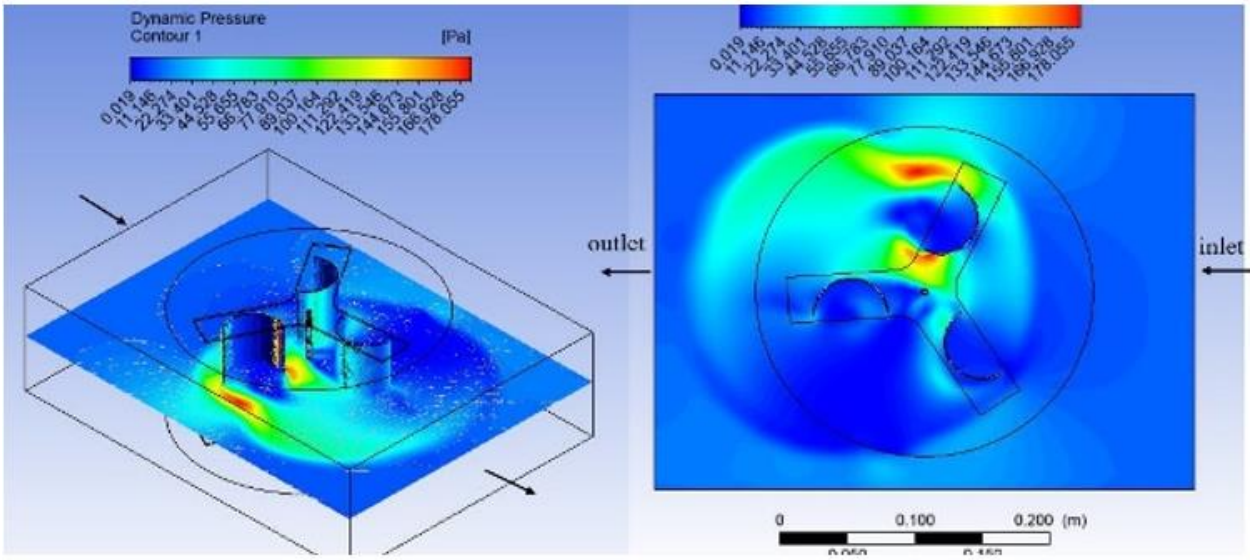

(b)

Edelweiss Applied Science and Technology
ISSN: 2576-8484
Vol. 9, No. 6: 2244-2260, 2025
DOI: 10.55214/25768484.v9i6.8364

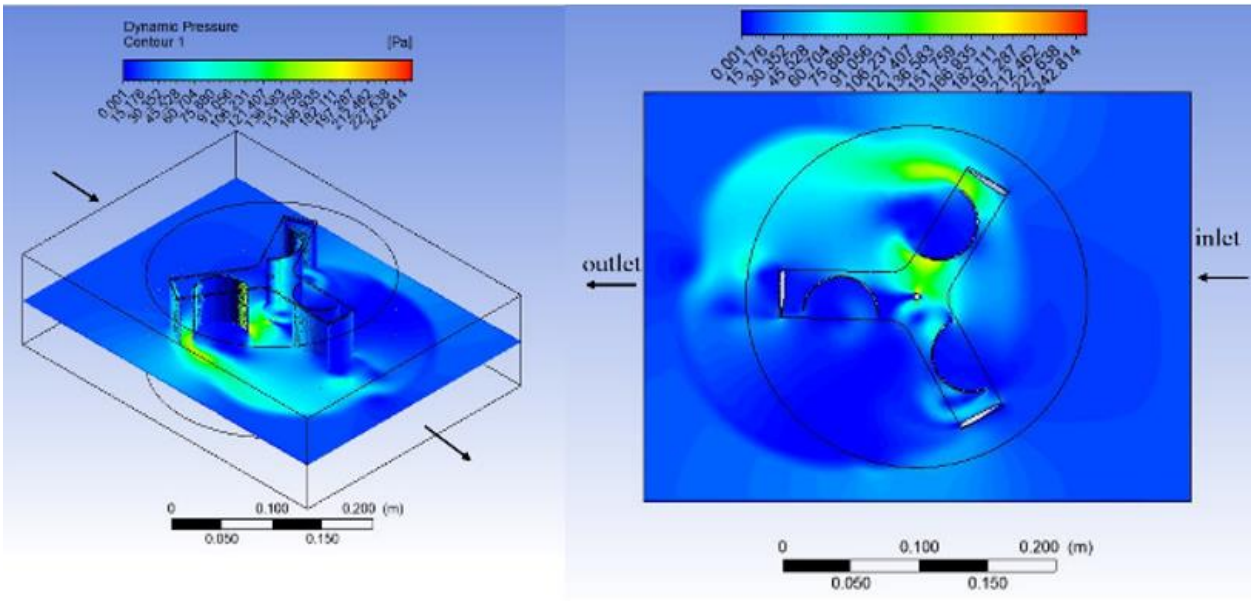

Figure 8.
Dynamic Pressure contour for wind turbine type (a) Darruis 3S-blades (b) Savonius (c) combined (Darrieus - Savonius).

Figure 9 illustrated the total pressure contour and velocity contour for Darrieus and combined wind turbine respectively.

Edelweiss Applied Science and Technology
ISSN: 2576-8484
Vol. 9, No. 6: 2244-2260, 2025
DOI: 10.55214/25768484.v9i6.8364

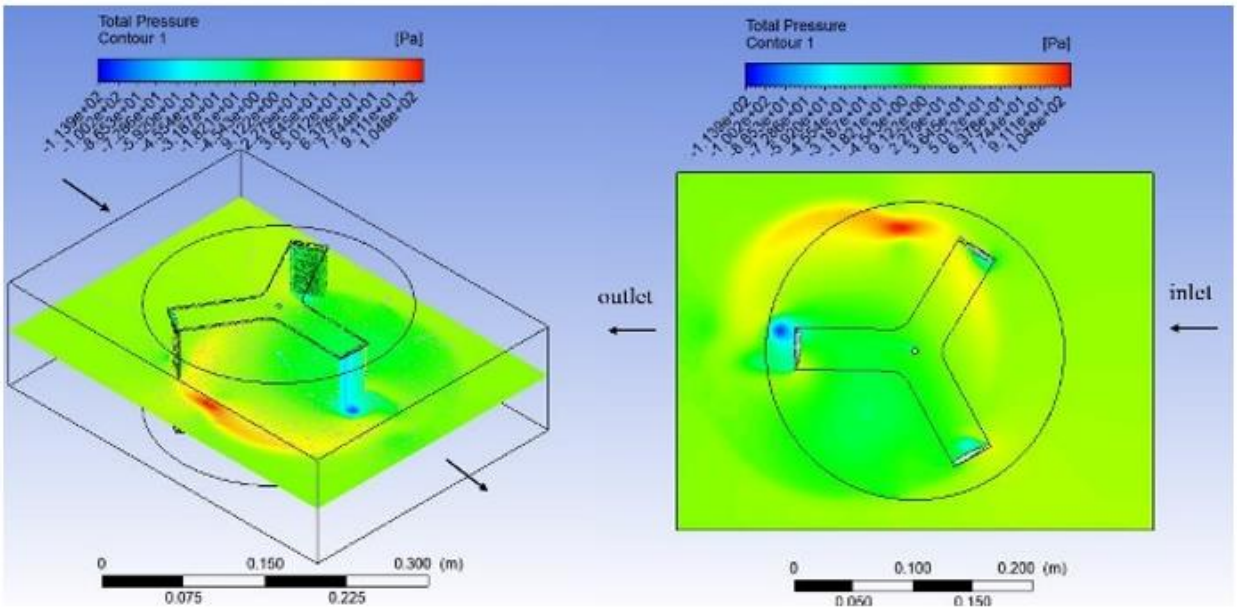

(a)

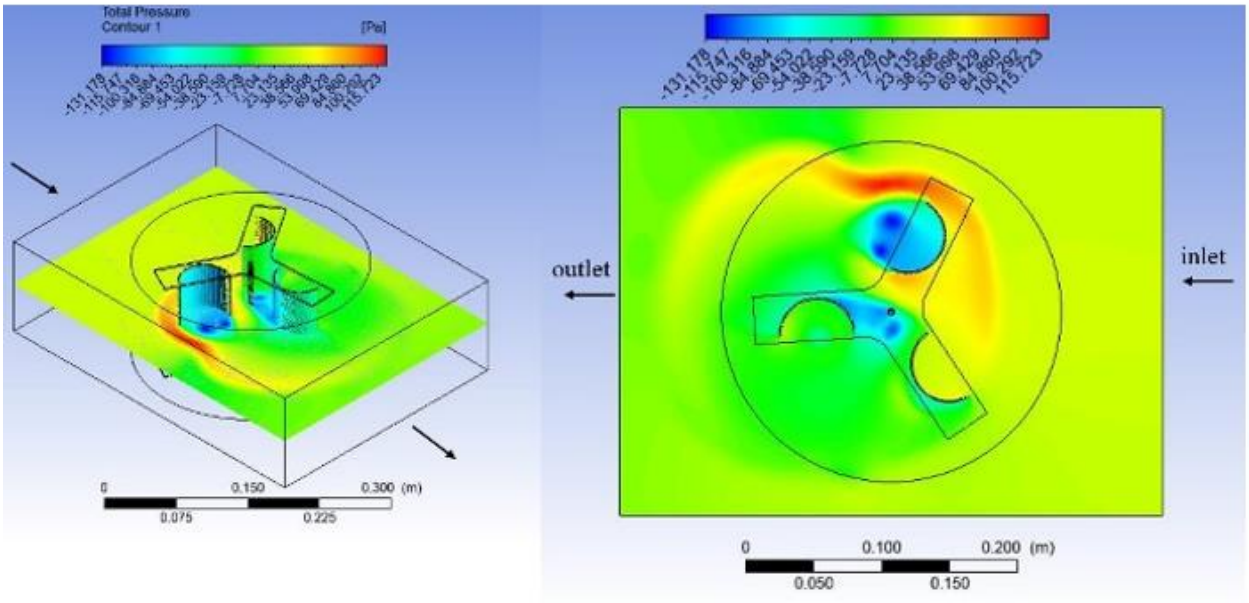

(b)

Edelweiss Applied Science and Technology
ISSN: 2576-8484
Vol. 9, No. 6: 2244-2260, 2025
DOI: 10.55214/25768484.v9i6.8364

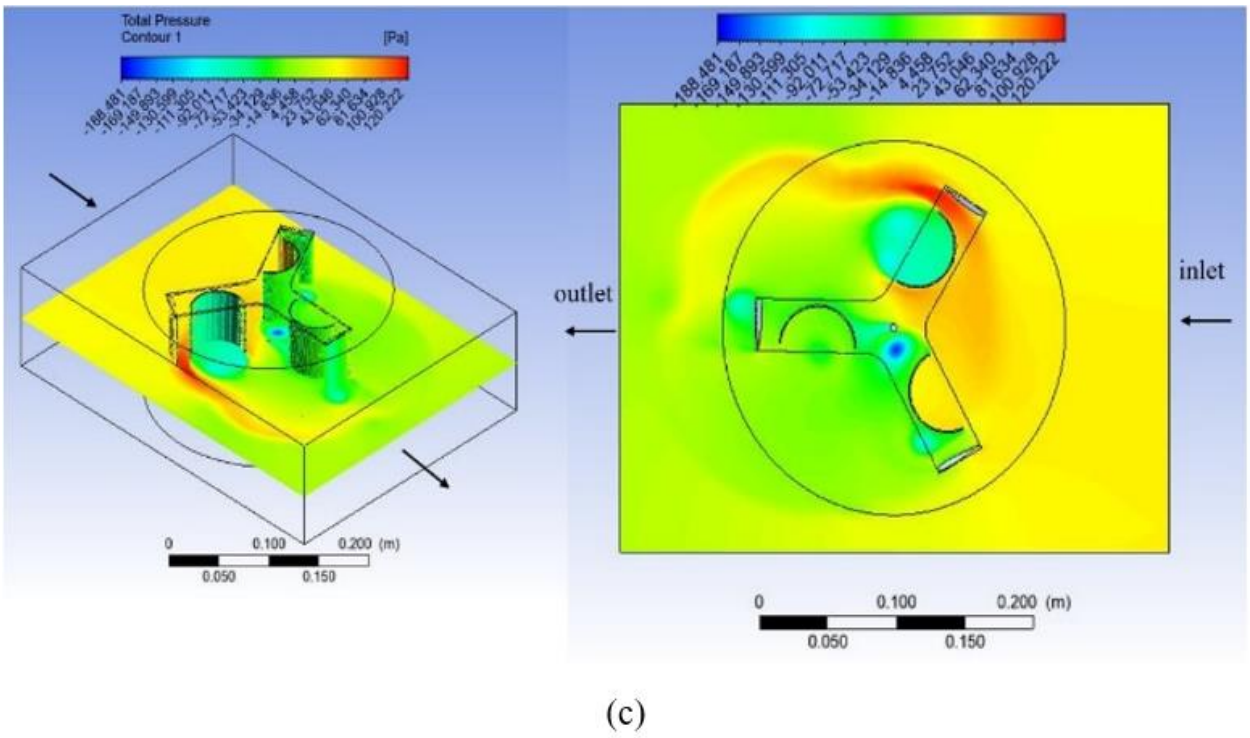

Figure 9.
Total Pressure Pressure contour for wind turbine type (a) Darruis 3S-blades (b) Savonius (c) combined (Darrieus - Savonius).

6. Results and Discussion

Figure 10 illustrates comparing the values of torque for the single 3SB-Darrieus wind turbine and a combined Darrieus-Savonius wind turbine. It can be seen from the figure that at a wind speed of 5 m/s, the highest torque was obtained for the single 3-blade Darrieus turbine and the 3-blade Darrieus-Savonius combined turbine, amounting to 0.0150 N.m and 0.0619 N.m, respectively. It is very clear from the figure that there is a noticeable improvement in the amount of rotational torque of the single Darrieus by using the Savonius blades by adding them to the rotating part of the Darrieus.

Edelweiss Applied Science and Technology
ISSN: 2576-8484
Vol. 9, No. 6: 2244-2260, 2025
DOI: 10.55214/25768484.v9i6.8364

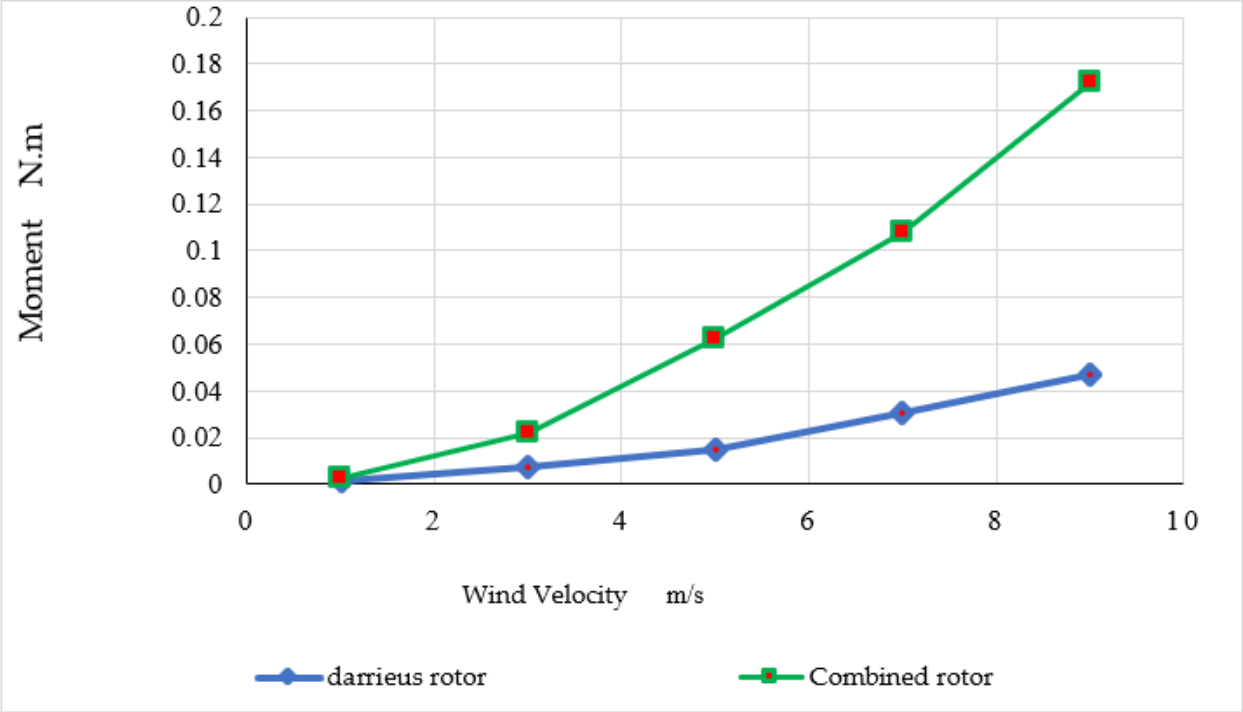

Figure 10.
Evaluation of torque with wind velocities for the single 3SB-Darrieus wind turbine and a combined Darrieus-Savonius wind turbine.

The power produced by each turbine has been examined by using the equation (4) as illustrated in figure11. It can be seen from the figure that at a wind speed of 5 m/s, the highest power was obtained for the single 3-blade Darrieus turbine and the 3-blade Darrieus-Savonius combined turbine, amounting to 0.754 watt and 3.0957 watt, respectively. It is very clear from the figure that there is a noticeable improvement in the amount of output power of the single Darrieus by using the Savonius blades by adding them to the rotating part of the Darrieus.

$$\text{Power} = T^{*}\,\omega \qquad (4)$$

Where: T: torque [N.m], ω: represented the angular velocity calculated by dividing the wind velocity by rotor radius ($\omega = V/r$).

Edelweiss Applied Science and Technology
ISSN: 2576-8484
Vol. 9, No. 6: 2244-2260, 2025
DOI: 10.55214/25768484.v9i6.8364

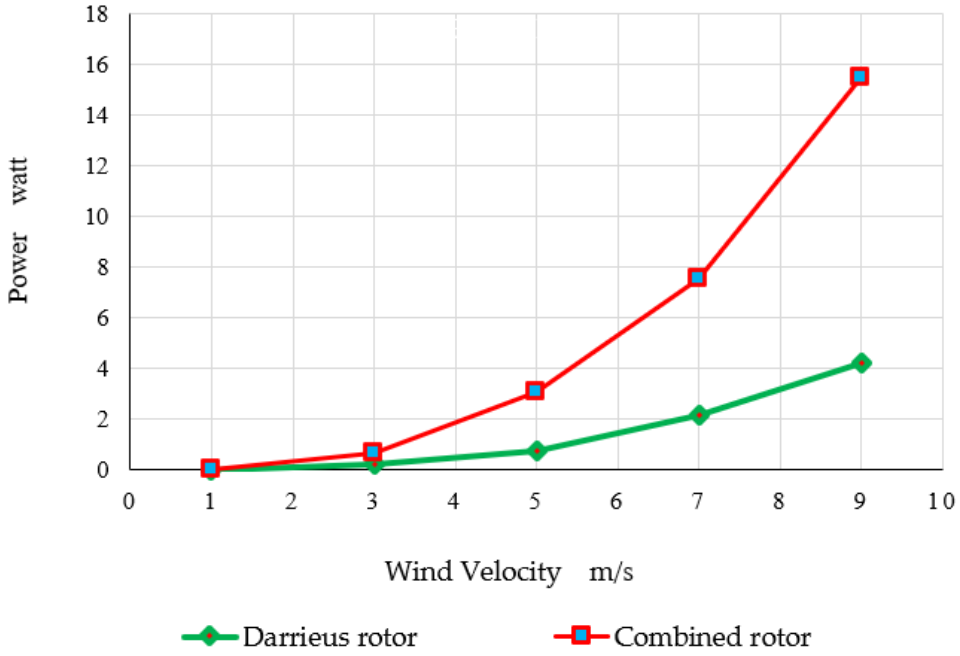

Figure 11.
Evaluation of power with different wind velocities for the single 3SB-Darrieus wind turbine and a combined Darrieus-Savonius wind turbine.

Figure 12 represents a comparison between the amounts of rotational torque of the integrated turbine with the rotational torque of the previous source [18] at a similar wind speed, the results showed that they were close for the two studies, which indicates verification of the results of the current study.

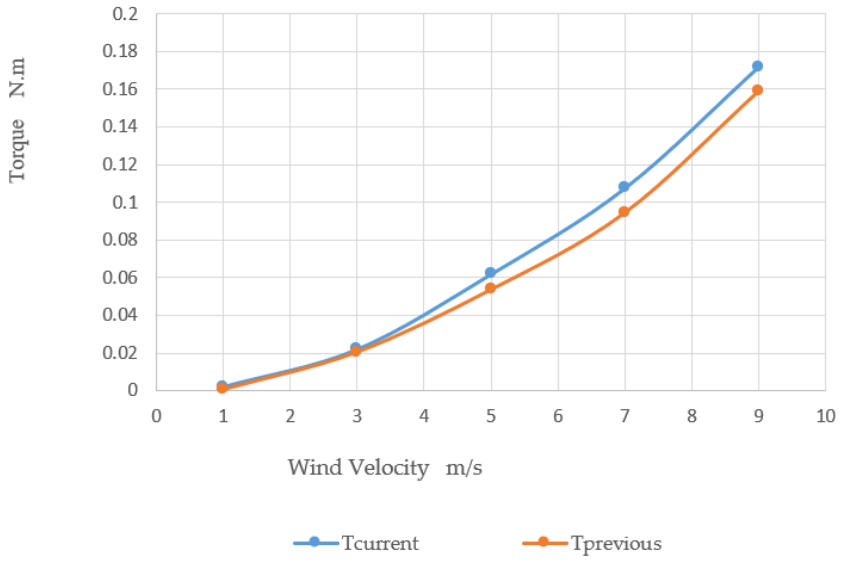

Figure 12.
Comparison between Tcurrent and Tprevious versus wind velocity.

Edelweiss Applied Science and Technology
ISSN: 2576-8484
Vol. 9, No. 6: 2244-2260, 2025
DOI: 10.55214/25768484.v9i6.8364

7. Conclusions

This study offers a numerical assessment of the aerodynamic performance and flow mechanics of a combined three-bladed Savonius and Darrieus turbine. Among the main markers derived from this numerical simulation are:

- The torque reached its maximum value in the combined wind turbine, exceeding the torque of the 3-bladed Darrieus wind turbine alone by up to 3%.
- The highest power obtained for the 3-bladed combined wind turbine is (3.0957) Watts, while for the 3-bladed Darrieus wind turbine is (0.754) Watts under the same wind speeds of 5 m/s, the results show a significant increase in the total power output of the combined wind turbine.
- An analysis comparing the combined wind turbines' rotational torque ratings with the rotational torque of the previous source [18] at a similar wind speed, the results showed that they were close for the two studies, which indicates verification of the results of the current study.

Transparency:

The authors confirm that the manuscript is an honest, accurate, and transparent account of the study; that no vital features of the study have been omitted; and that any discrepancies from the study as planned have been explained. This study followed all ethical practices during writing.

References

[1] G. W. E. C. (GWEC), *Global wind 2006 report*. Brussels, Belgium: GWEC, 2006.

[2] R. Gupta and A. Biswas, "CFD analysis of flow physics and aerodynamic performance of a combined three-bucket Savonius and three-bladed Darrieus turbine," *International Journal of Green Energy*, vol. 8, no. 2, pp. 209-233, 2011. https://doi.org/10.1080/15435075.2011.561358

[3] A. Bahaj, L. Myers, and P. James, "Urban energy generation: Influence of micro-wind turbine output on electricity consumption in buildings," *Energy and Buildings*, vol. 39, no. 2, pp. 154-165, 2007. https://doi.org/10.1016/j.enbuild.2006.04.015

[4] S. Mertens, *Wind energy in the built environment*. United Kingdom: Multiscience Publishing, 2006.

[5] M. Ragheb, *Vertical axis wind turbines* California: Sandia National Laboratories, 2015.

[6] I. Paraschivoiu, *Wind turbine design with emphasis on Darrieus concept*. Canada: Polytechnic International, 2002.

[7] M. Islam, D. S.-K. Ting, and A. Fartaj, "Aerodynamic models for Darrieus-type straight-bladed vertical axis wind turbines," *Renewable and Sustainable Energy Reviews*, vol. 12, no. 4, pp. 1087-1109, 2008. https://doi.org/10.1016/j.rser.2007.01.018

[8] K. Seki, "Research and development of high-performance airfoil sections for vertical axis wind turbines at low Reynolds number," *Transactions of the Japan Society of Mechanical Engineers*, vol. 57, no. 536, pp. 1297–1304, 1991. https://doi.org/10.1299/jsme1958.57.1297

[9] L. Yan, "Lecture on the technology of vertical-axis wind turbine (IV)," *Renewable Energy Resources*, vol. 27, no. 4, pp. 121–123, 2009. https://doi.org/10.1016/j.renene.2008.07.008

[10] M. H. M. Hafidzal, W. M. F. W. Mahmood, M. Z. A. Manaf, M. S. Zakaria, M. N. A. Saadun, and M. N. A. Nordin, "Soot particle trajectories of a Di diesel engine at 18 ATDC crankshaft angle," presented at the In IOP Conference Series: Materials Science and Engineering, IOP Publishing, 2013.

[11] A. A. Basri *et al.*, "The hemodynamic effects of paravalvular leakage using fluid-structure interaction: Transcatheter aortic valve implantation patient," *Journal of Medical Imaging and Health Informatics*, vol. 6, no. 6, pp. 1513–1518, 2016. https://doi.org/10.1166/jmihi.2016.1805

[12] A. G. Ihsan, A. K. Farhan, W. M. Ahmed, and K. H. Ahmed, "MHD natural convection in a fully opened parallelogrammic enclosure filled with copper–water nanofluid and partially heated from its left sidewall," *Journal of Advanced Research in Fluid Mechanics and Thermal Sciences*, pp. 1–10, 2020.

[13] A. K. Farhan, T. M. Ayad, and N. K. Abdul Jabbar, "Temperature Stratification in a thermal storage tank: the effect of flow rate and aspect ratio," *Journal of Engineering Science and Technology*, vol. 16, no. 2, pp. 1066-1081, 2021.

[14] H. Gad, A. Abd El-Hamid, W. El-Askary, and M. Nasef, "A new design of savonius wind turbine: numerical study," *CFD letters*, vol. 6, no. 4, pp. 144-158, 2014.

[15] A. K. Farhan and A. H. Omar, "The effect of the blade shapes on the drag force of vertical axis wind turbine," *journal of Engineering Science and Technology*, vol. 18, no. 6, pp. 2736 – 2747, 2023.
[16] A. M. Biadgo, A. Simonovic, D. Komarov, and S. Stupar, "Numerical and analytical investigation of vertical axis wind turbine," *FME Transactions*, vol. 41, no. 1, pp. 49-58, 2013.
[17] A. K. Farhan, "Numerical investigations on aerodynamic characteristics of a three-bladed combined Darrieus-vane type wind turbine," *Journal of Engineering Science and Technology*, vol. 18, no. 3, pp. 1762 – 1774, 2023.
[18] A. H. Omar and A. K. Farhan, "Development of initial torque for darrieus vertical axis wind Turbine," *International Journal of Latest Engineering and Management Research* vol. 08 no. 03, pp. 95-100, 2023.

Edelweiss Applied Science and Technology
ISSN: 2576-8484
Vol. 9, No. 6: 2244-2260, 2025
DOI: 10.55214/25768484.v9i6.8364